JCI insight

RESEARCH ARTICLE

Human adipose tissue microvascular endothelial cells secrete PPARγ ligands and regulate adipose tissue lipid uptake

Silvia Gogg,[1] Annika Nerstedt,[1] Jan Boren,[2] and Ulf Smith[1]

[1]Lundberg Laboratory for Diabetes Research and [2]Wallenberg Laboratory, Department of Molecular and Clinical Medicine, Sahlgrenska Academy, University of Gothenburg, Gothenburg, Sweden.

Human adipose cells cannot secrete endogenous PPARγ ligands and are dependent on unknown exogenous sources. We postulated that the adipose tissue microvascular endothelial cells (aMVECs) cross-talk with the adipose cells for fatty acid (FA) transport and storage and also may secrete PPARγ ligands. We isolated aMVECs from human subcutaneous adipose tissue and showed that in these cells, but not in (pre)adipocytes from the same donors, exogenous FAs increased cellular PPARγ activation and markedly increased FA transport and the transporters FABP4 and CD36. Importantly, aMVECs only accumulated small lipid droplets and could not be differentiated to adipose cells and are not adipose precursor cells. FA exchange between aMVECs and adipose cells was bidirectional, and FA-induced PPARγ activation in aMVECs was dependent on functional adipose triglyceride lipase (ATGL) protein while deleting hormone-sensitive lipase in aMVECs had no effect. aMVECs also released lipids to the medium, which activated PPARγ in reporter cells as well as in adipose cells in coculture experiments, and this positive cross-talk was also dependent on functional ATGL in aMVECs. In sum, aMVECs are highly specialized endothelial cells, cannot be differentiated to adipose cells, are adapted to regulating lipid transport and secreting lipids that activate PPARγ, and thus, regulate adipose cell function.

Introduction

The adipose tissue plays a key role in regulating whole-body energy homeostasis through storage and release of lipids according to need. In humans, the subcutaneous adipose tissue (SAT) is the largest and best site to store excess lipids and release them according to needs (1, 2). SAT is also an important regulator of whole-body insulin sensitivity by preventing ectopic lipid accumulation and through its thermogenic and endocrine functions (1, 3, 4).

Most studies of adipose tissue function and metabolism have focused on the adipose cells, but recent studies have also emphasized the importance of stromal vascular cells, including progenitor and inflammatory cells (4, 5).

Very little is known about the role of the abundant microvascular endothelial cells in the adipose tissue apart from their critical role in regulating angiogenesis, essential for normal adipose tissue expansion (6, 7). However, by virtue of providing a barrier between the blood and adipose tissue cells, they must also be important regulators of lipid transport to and from the bloodstream. In support of this, it was recently shown that inducing apoptosis in adipose endothelial cells with specific peptides reduced both obesity and insulin resistance in obese monkeys (8). Furthermore, a recent extensive study showed that endothelial cells and adipose cells can cross-talk through the release of extracellular vesicles regulated by glucagon, sphingomyelinase, and ceramide generation (9). In agreement with this, it was previously shown that the adipose tissue is a rich source of systemic trafficking of extracellular vesicles targeting other tissues (10).

Two principal mechanisms for fatty acid (FA) transport have been described: the diffusion model with a rapid rate of FA "flip-flop" across the plasma membrane independent of proteins (11, 12) and the facilitated, protein-mediated mechanism (13, 14). However, the precise mechanisms by which different tissues take up FAs are still under debate.

PPARγ is the key regulator of adipose cell differentiation and ability to store lipids and the synthetic PPARγ agonists, the thiazolidinediones (TZDs), and to lower free FA levels in humans, primarily by

Conflict of interest: The authors have declared that no conflict of interest exists.

Submitted: October 31, 2018
Accepted: January 25, 2019
Published: March 7, 2019

Reference information:
JCI Insight. 2019;4(5):e125914.
https://doi.org/10.1172/jci.insight.125914.

directing lipids into the adipose tissue and away from liver and muscle and, thereby, improving insulin resistance. The adipose cells require PPARγ activation, and human cells, in contrast with murine 3T3-L1 cells (15, 16), are unable to secrete endogenous PPARγ ligands and are dependent on exogenous TZD sources for differentiation in vitro (17). However, nothing is known about the in vivo situation and the presence of endogenous PPARγ ligands. Interestingly, genetic animal models have also documented the importance of PPARγ in the endothelial cells for peripheral lipid uptake (18, 19). Obese mice lacking endothelial PPARγ have increased circulating free FA levels and decreased expression of the lipid transporters FA translocase (FAT/CD36) and FA-binding protein 4 (FABP4) in peripheral tissues (18, 19). The positive effects of exogenous PPARγ ligands in increasing lipid uptake and FA transporters in human endothelial cells have also recently been reported (20).

Adipose triglyceride lipase (ATGL) plays a key role for lipid droplet degradation in adipocytes and nonadipocyte cells and exhibits high specificity for triglycerides (21, 22). Apart from regulating lipolysis in response to cAMP activation, ATGL may also play a role in the formation of lipid activators of PPARα in the heart (23) and liver (24, 25).

In this study, we isolated and purified primary microvascular endothelial cells (aMVECs) from human SAT needle biopsies, using our previously reported method (26), to examine FA transport and potential cross-talk between purified aMVECs and preadipocytes (PAs) in the stromal vascular cell fraction isolated from the same donors. Our data show an intimate cross-talk between these cells and that aMVECs regulate adipose tissue FA transport as well as adipose cell PPARγ activation through functional ATGL in aMVECs.

Results

We first examined FA transport in purified aMVECs and its regulation through ambient FA levels, focusing on potential long-term effects of elevated ambient FA levels as seen in obesity and type 2 diabetes (T2D).

Figure 1A shows basal uptake and that the presence of 300 μM oleic acid (OA), the major circulating FA in humans, for 24 hours increased transport several-fold in aMVECs. Thus, aMVECs adapt to the ambient FA levels in their ability to transport FA, suggesting that human conditions with increased FA levels are associated with enhanced transport capacity across the aMVECs to and from the adipose cells.

PPARγ and FA regulate lipid transporters in aMVECs but not in HUVECs or cardiac microvascular cells. To further address this, we tested whether aMVECs are specialized and differ from other microvascular or macrovascular cells. We examined the regulation of the key lipid transporters FABP4 and CD36 in human macrovascular HUVECs, aMVECs, and human microvascular cardiac-derived endothelial cells (cMVECs). Both of these transporters were robustly expressed at the transcription level, but neither OA nor the PPARγ ligand rosiglitazone (ROSI) affected their transcript or protein levels in HUVECs, while aMVECs were clearly responsive to both, including for PPARγ activation (Figure 1, B–D). Human cMVECs, like HUVECs, did not respond to OA for transcriptional activation of either PPARγ or FA transporters (Figure 1G). Thus, the difference in regulation by FA is because of tissue source, rather than micro- or macrovascular origin, and shows that aMVECs are specialized in their response to FAs. Because both *FABP4* and *CD36* are well-established PPAR-responsive genes (14, 17), these data suggest that OA activates PPARγ in aMVECs but not in macrovascular HUVECs or microvascular cMVECs.

This effect of OA in aMVECs was both time and concentration dependent. It was quite rapidly induced, requiring around 4 hours but then further increasing over the 48-hour exposure time. As shown by the concentration curves in Supplemental Figure 1, A–D (supplemental material available online with this article; https://doi.org/10.1172/jci.insight.125914DS1), oleic and palmitic acid as well as the short-chain FA octanoate significantly increased the expression of *FABP4*, *CD36*, and *PPARγ* in aMVECs. A similar effect was seen with the unsaturated omega-3 FA α-linolenic acid (Supplemental Figure 1E). Thus, long-chain FAs, independent of degree of saturation, induce PPARγ and lipid transporters in aMVECs while macrovascular HUVECs and cMVECs are unresponsive.

Of note, there was no additive effect of OA and ROSI in aMVECs, suggesting that the effect of OA was mediated through PPARγ activation. This was also confirmed by the finding that 2 specific PPARγ inhibitors, GW9662 and T0070907(Figure 1, E and F), completely inhibited the effect of both OA and ROSI on *FABP4* and *CD36* activation. Thus, microvascular aMVECs show marked differences in their regulation by FA and ability to respond with PPARγ activation compared with other macro/microvascular endothelial cells. As shown in Figure 1I, aMVECs were also characterized by high endogenous transcriptional levels of *PPARγ*.

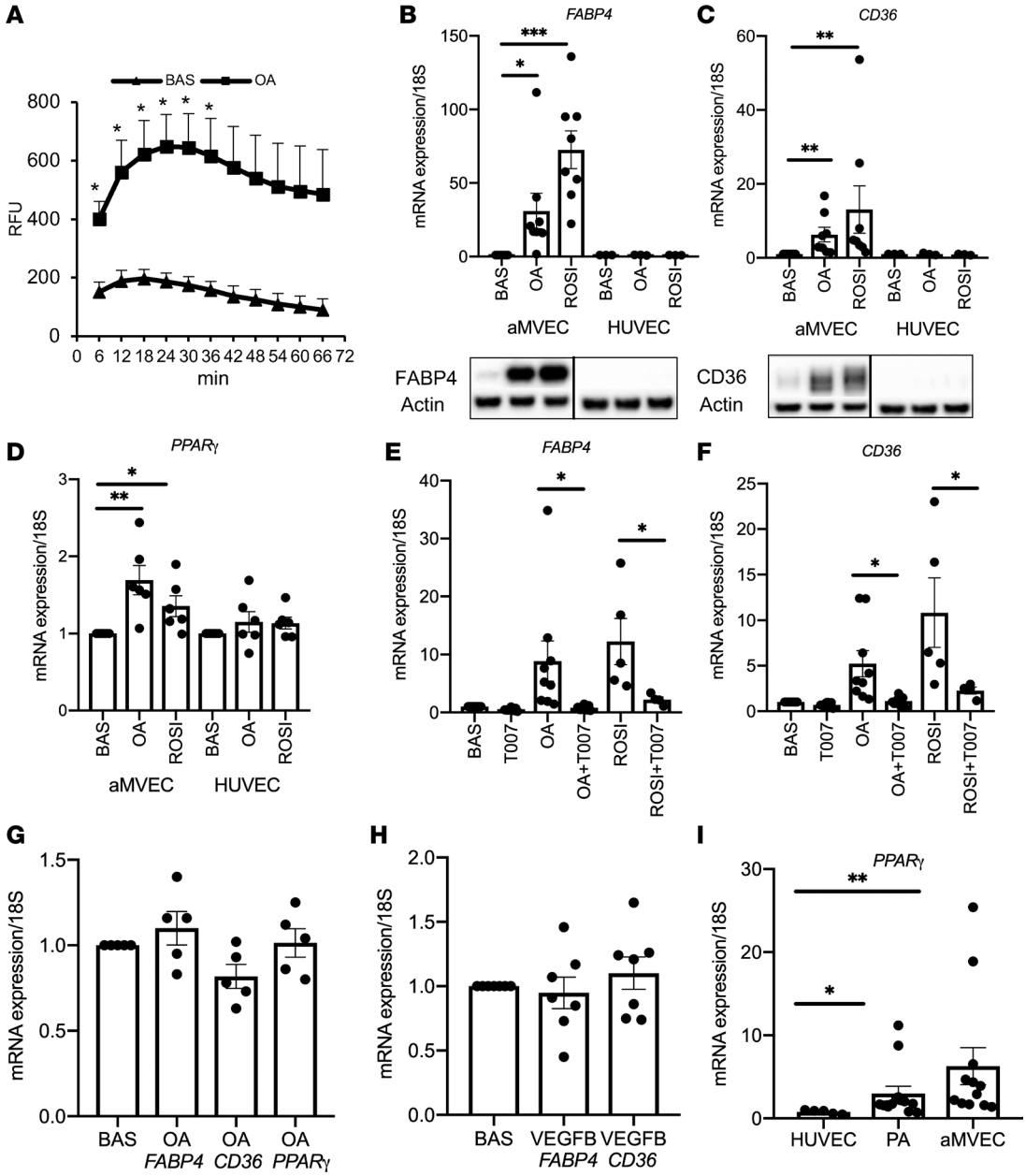

Figure 1. Effects of free fatty acids (FA). (**A**) FA transport: aMVECs were incubated for 24 hours without (basal condition; BAS) or with 300 μM OA followed by 60 minutes starvation, but with maintained OA, as indicated. The FA transport assay (Quencher-Based Technology assay) was performed as described in Methods. The results, expressed as relative fluorescence units (RFU), are the means of data from 4 experiments. *$P < 0.05$ compared with BAS. (**B**–**D**) Regulation of lipid transporters: aMVECs and HUVECs were incubated without (BAS) or with 300 μM OA or 5 μM ROSI for 24 hours. Quantitative real-time PCR (qRT-PCR) of FABP4 (**B**), CD36 (**C**), and PPARγ (**D**) expressed as mRNA/18S rRNA ratio; $n = 8$ aMVECs or $n = 5$ HUVECs. *$P < 0.05$; **$P < 0.01$; ***$P < 0.001$ compared with BAS. (**B** and **C**) The bottom images show representative Western blots of the protein level of FABP4 (**B**) and CD36 (**C**). (**E** and **F**) Effect of a PPARγ inhibitor in aMVECs: Cells were incubated for 24 hours without (BAS) or with 300 μM OA or 5 μM ROSI, alone or in the presence of 1 μM T0070907(T007). qRT-PCR of FABP4 (**E**) and CD36 (**F**); $n = 6$. *$P < 0.05$ compared with OA alone. (**G**) OA in cMVECs: The cardiac microvascular cells were starved and incubated without (BAS) or with 300 μM OA for 24 hours. qRT-PCR of CD36, FABP4, and PPARγ, $n = 5$. (**H**) Effect of VEGF in aMVECs: Cells were starved and incubated without (BAS) or with 100 μM hrVEGF-B for 24 hours. qRT-PCR in aMVECs for CD36 and FABP4; $n = 7$. (**I**) Comparative mRNA expression of PPARγ in HUVECs, PAs, and aMVECs. Data are from at least 5 experiments. *$P < 0.05$; **$P < 0.01$ compared with HUVECs. In all graphs bars represent mean ± SEM. Wilcoxon's signed-rank test (**A**), Kruskal-Wallis test (**B**–**D** and **G**–**I**), and 1-way ANOVA (**E** and **F**).

To further verify specificity in the regulation of lipid transporters, we examined whether aMVECs were responsive to VEGF-B, previously shown to regulate lipid transport in microvascular endothelial cells from skeletal muscle and heart (13, 27), but saw no such effects (Figure 1H).

aMVECs are not adipose precursor cells. Adipose precursor cells are closely associated with vascular cells (28), and adipose cells can grow from cultured, intact human adipose tissue biopsies (29). Thus, we examined whether these purified $CD31^+$ aMVECs could become adipose cells by incubating them with adipogenic differentiation cocktail or OA for several days. Although they could clearly accumulate many small lipid droplets when incubated with OA (Figure 2, B and E), this was not induced by the differentiation cocktail alone (Figure 2I) and no lipids were accumulated in the absence of OA (Figure 2H), contrasting with the expected effect seen in PAs (Figure 2, F and G). Furthermore, the cells never accumulated large lipid droplets or expressed markers of specific adipogenic differentiation, such as CCAAT/enhancer-binding protein α (*CEBPα*) and glucose transporter 4 (*GLUT4*) (Figure 2, J–N). In addition, aMVECs did not express PPARγ2 (data not shown). Thus, we conclude that the aMVECs are not adipogenic precursor cells but do express some "adipose-like" markers, supporting that they are specialized and adapted to the function of the adipose tissue.

Uptake and release of lipids by aMVECs. To further characterize the integrated function of aMVECs, we incubated the cells without or with OA for up to 48 hours. During the last 24 hours, we also added the lipolytic agent forskolin to examine whether this reduced the accumulated triglycerides. The microphotographs in Figure 2, A–E, show aMVECs stained with Oil Red O. No or only few lipids were revealed by Oil Red O staining in the BAS (Figure 2A) whereas clear staining shows the presence of accumulated triglycerides in cells treated with OA (Figure 2, B and E). When forskolin was added to OA-treated cells during the last 24 hours, the cells lost their previously accumulated lipids (Figure 2D, OA + forskolin), but they remained in cells not treated with forskolin (Figure 2B). Quantification of lipid surface area showed an approximately 13-fold increase in cells incubated with OA, and this surface area was reduced by approximately 80% with forskolin (Figure 2D). Cells continuously exposed to OA also had clear small lipid droplet accumulation (Figure 2E) but never differentiated to adipose cells.

aMVEC adipocytes cross-talk in regulating lipid compartmentalization. To further characterize the interaction between aMVEC and SAT adipocytes, we performed coculture experiments using 2 experimental designs (Figure 3, A and B). aMVECs or partially differentiated PAs were preloaded with BODIPY to allow the identification of FAs (Figure 3, C and D, microphotographs). The cells were then carefully washed before the coculture insert was introduced. As shown in Figure 3D (microphotographs), preloading the adipocytes allowed BODIPY uptake in aMVECs and vice versa from BODIPY preloaded aMVEC into adipocytes (Figure 3C). aMVECs accumulate many small lipid droplets, which are released and taken up by the PAs and accumulated in their large droplets. No direct quantification of lipid accumulation was performed, but additional experiments were performed with similar results, as shown in Supplemental Figure 2, A and B. These data support the expected intimate bidirectional cross-talk between the adipose cells and aMVECs in release and uptake of FAs.

OA does not activate PPARγ or FA transporters in PAs. In contrast with aMVECs, the presence of OA for 24 hours or longer did not increase the transcriptional activation of *CD36*, *FABP4*, or *PPARγ* in PAs whereas the cells were, as expected, responsive to PPARγ ligands (Figure 4, A–C). Thus, FA uptake by the PA is primarily regulated at the substrate level and by exogenous PPARγ ligands.

Effects of aMVECs on PA differentiation and PPARγ activation. The potential role of the intimate cross-talk between the human PAs and aMVECs in also activating PPARγ in the adipose cells was then addressed. This is an important question because human PAs are dependent on an external PPARγ ligand for differentiation and lipid storage (17) and, thus, are unable to induce or secrete endogenous PPARγ ligands in contrast with murine 3T3-L1 cells (16).

To directly test the cross-talk between these cells, we performed Thincerts cocultures with human PAs and aMVECs, examining the effect on *PPARγ* and *FABP4* in the PAs. PAs were cultured for 48 hours, and inserts with cultured aMVECs were then added on top of the PAs for an additional 48 hours. The graphs in Figure 4, D and E, show that aMVEC inserts significantly increased the transcriptional activation of *FABP4* and *PPARγ* in PAs. The degree of activation of *PPARγ* was related to the phenotype of the donor such that the medium released by aMVECs from obese donors activated PPARγ to a greater extent than cells or medium from lean donors (Figure 4F).

To further validate the presence of PPARγ agonist(s) in the supernatants of cultured aMVECs, we examined the effect of the culture medium in the cell-based PPARγ reporter assay GeneBLAzer. As shown in Figure 4G, aMVEC-conditioned medium significantly increased PPARγ activation in the

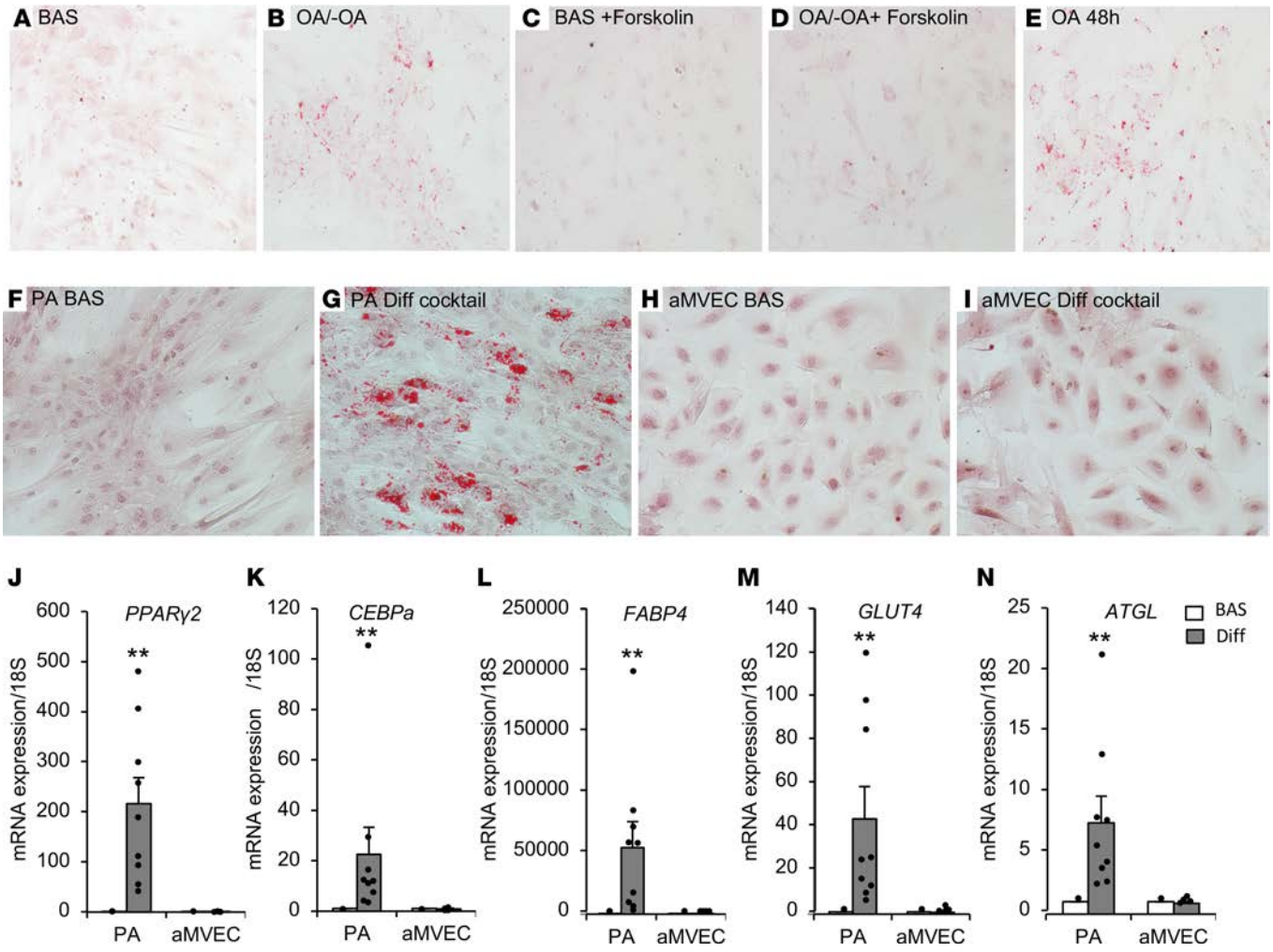

Figure 2. aMVECs take up and release lipids but are not adipose precursor cells. (**A**–**E**) Lipolytic effect of forskolin in aMVECs: Cells were treated for 24 hours without (BAS) or with 300 μM OA. During the last 24 hours of incubation, OA was removed (**B** and **D**) or not (**E**), and the cells were exposed to 10 μM forskolin for an additional 24 hours (**C** and **D**). The intracellular lipid accumulation was revealed by Oil Red O staining (original magnification, ×100). (**F**–**N**) aMVECs are not adipose precursor cells. PAs and aMVECs were incubated with or without an adipogenic differentiation (Diff) cocktail for 7 days. (**F**–**I**) The presence of lipids was revealed with Oil Red O staining (original magnification, ×100). (**J**–**N**) The genes, as indicated in the figures, were analyzed with qRT-PCR. Data are from at least 4 experiments. $^{**}P < 0.01$. Bars represent mean ± SEM. Wilcoxon's signed-rank test.

reporter cells (PPARγ-UAS-bla HEK 293H cells), an effect that was further enhanced by the presence of OA in the culture media, which activated PPARγ to a similar extent as 1 nM ROSI (Figure 4H). However, we did not see this when we incubated the cells with media from the cultured PAs from the same donors (Figure 4G). Although the nature of the secreted PPARγ ligands is currently under investigation, recovery of PPARγ activation in lipid medium extracts supports that they are lipids. This is further supported by the direct enhancing effect of FAs in aMVECs and the importance of aMVEC ATGL in mediating this effect, as discussed below.

To further validate the role of FAs in inducing endogenous and secreted PPARγ ligands in aMVECs, we examined whether the free FA receptor 1–specific (FFAR1- or GPR40-specific) and modified FA ligand GW9508 exerted similar effects as OA and other FAs in aMVECs. As shown in Figure 5, A and B, GW9508 was even more potent than OA in enhancing *PPARγ* and *FABP4* in aMVECs. In addition, human PAs responded to GW9508 (Figure 5, C and D) but not to OA, as discussed, showing that modified FAs can be PPARγ ligands in both cell types while only aMVECs directly respond to native FAs.

We then examined mechanisms for the effects of FAs, focusing on documenting the regulatory effect of PPARγ itself and the importance of ATGL and hormone-sensitive lipase (HSL) in generating ligands and activating PPARγ.

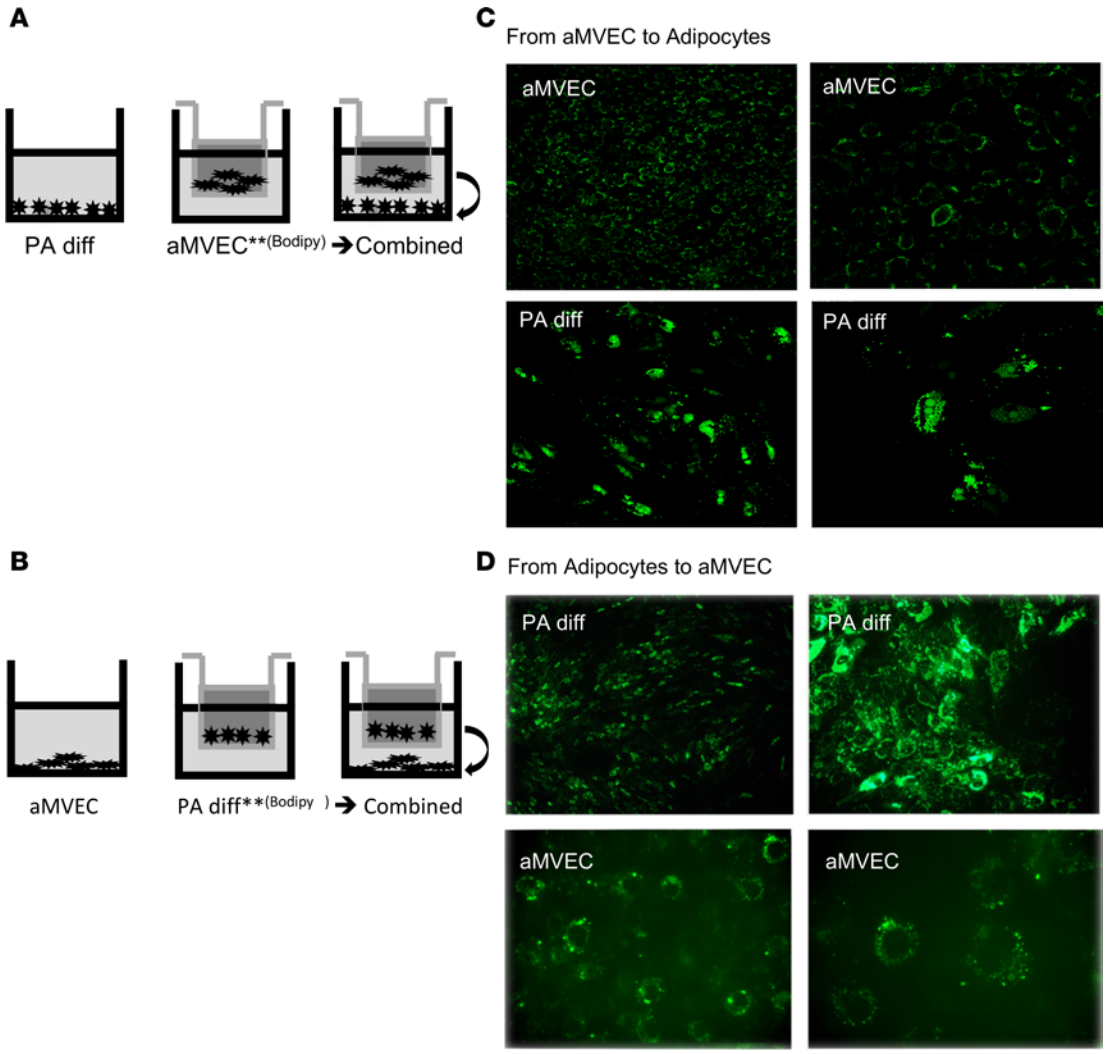

Figure 3. aMVEC/adipocyte cross-talk. (**A** and **B**) Experimental design with Thincert coculture with the long-chain FA analog fluorescent BODIPY-500/510 C1, C12: Adipocytes and aMVECs were independently seeded in the bottom of a culture dish or on the insert membrane. **BODIPY was added to the monocultures and then combined with the opposite unlabeled population, as shown in the schematic figures. (**C** and **D**) Microphotographs showing aMVECs and adipocytes cross-talk. aMVECs previously exposed to OA and partially differentiated PAs were grown independently as described. The differentiated PAs (PA diff) and aMVECs filled with lipids were incubated with 3 μM fluorescent BODIPY for 3 hours (upper microphotographs). After a thorough wash of the excess label with PBS, the labeled and not labeled cells were paired as shown in the figures (**A**) and (**B**), and the microphotographs were taken after 48 hours of coculture (bottom microphotographs). Original magnification, ×100 (left); ×400 (right).

PPARγ is critical for endogenous FABP4 and CD36 activation by OA and GPR40 ligand in aMVECs. To further validate the importance of PPARγ in regulating the FA transporters, we silenced PPARγ in aMVECs, and this significantly inhibited the effects of both OA and GW9508 on FABP4 and CD36 (Figure 6, A–D). Similar results were found for the PPARγ ligand ROSI (Figure 6, E–G).

These results confirm that PPARγ plays a critical role in mediating the effect of both OA and the modified lipid ligand GW9508 in enhancing lipid transport in aMVECs.

ATGL is critical for endogenous PPARγ, FABP4, and CD36 activation by OA and GPR40 ligand. OA increased lipid droplet formation in aMVECs, and these were reduced by cAMP activation (Figure 2), supporting the importance of ATGL. OA also increased ATGL protein in aMVECs (Figure 7A). To examine the importance of aMVEC lipolysis, we silenced ATGL in aMVECs, and this completely inhibited the positive effect of OA on PPARγ and the PPARγ-regulated lipid transporters (Figure 7, A–E). Interestingly, basal PPARγ protein was also reduced, supporting a constitutive effect of ATGL on endogenous PPARγ expression in aMVECs. In addition, the positive effect of the GPR40 agonist GW9508 on these transporters was markedly inhibited by silencing ATGL (Figure 7, G–J). To exam-

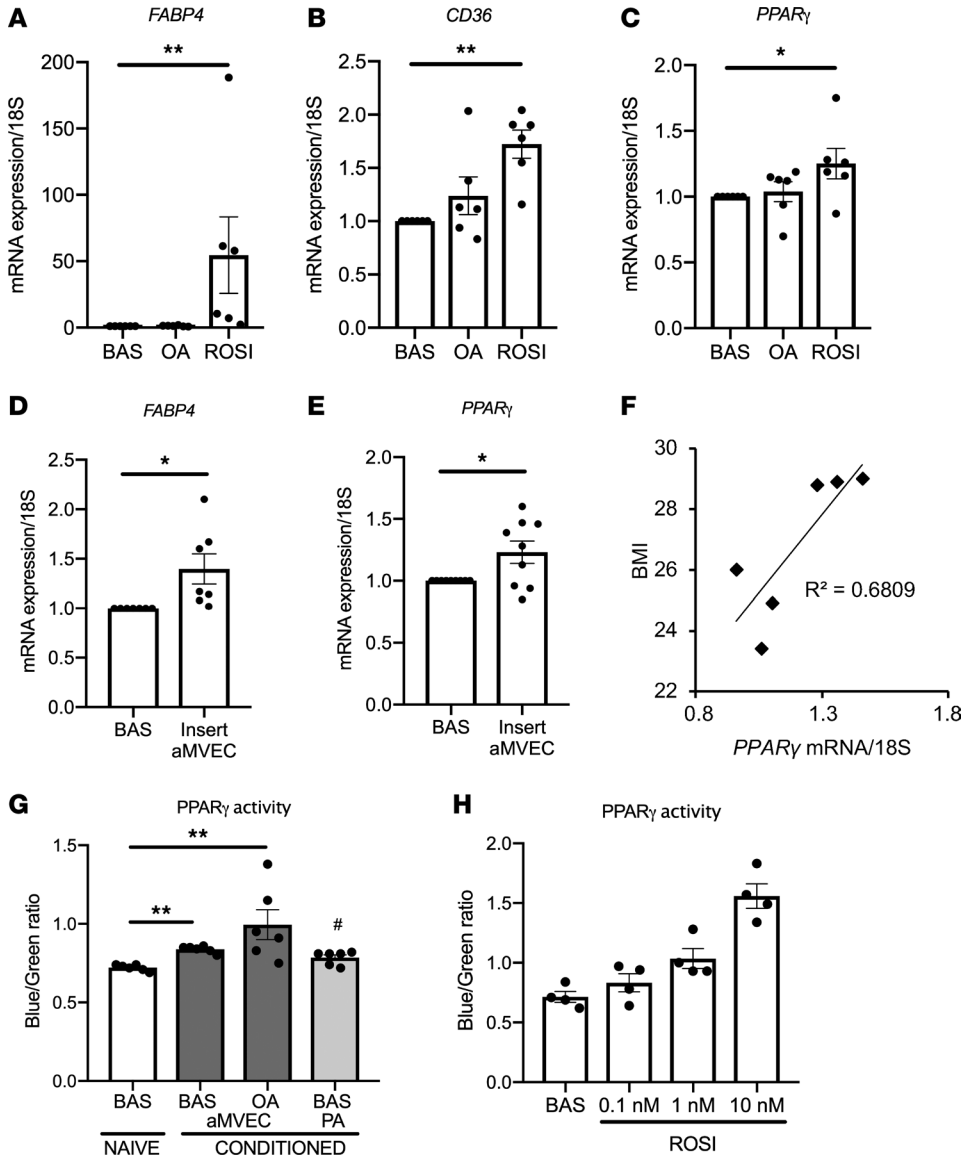

Figure 4. Effect of OA in PAs. (**A**–**C**) Human PAs were starved and incubated without (BAS) or with 300 μM OA or 5 μM ROSI for 24 hours. qRT-PCR of FABP4 (**A**), CD36 (**B**), and PPARγ (**C**); $n = 6$. $^{*}P < 0.05$; $^{**}P < 0.01$ compared with BAS. (**D**–**F**) aMVECs and PAs cross-talk. aMVECs and PAs were grown independently either in cell culture dishes or in cell culture inserts for 48 hours. PAs were cocultured with the aMVEC insert or without (BAS) for an additional 48 hours. qRT-PCR of FABP4, where $n = 8$ (**D**), and PPARγ, where $n = 6$ (**E**). $^{*}P < 0.05$. (**F**) Correlation between PPARγ expression and donor's BMI; $n = 6$, and $P < 0.05$. Pearson's correlation. (**G** and **H**) PPARγ activation: PPARγ-UAS-bla HEK 293H cells were plated in a 384-well plate and cultured for 20 hours with aMVEC- or PA-conditioned medium obtained after 24 hours of incubation. Naive medium was used as a control. After the incubation time the assay was resolved as described in Methods, and the fluorescence emission values at 460 nm (blue) and 530 nm (green) were obtained after 90 minutes using a fluorescence plate reader. (**G**) The bars show the blue/green ratio after background subtraction (medium only, without cells) for each condition tested; $n = 6$. $^{*}P < 0.05$; $^{**}P < 0.01$ compared with naive medium; $^{\#}P < 0.05$ compared with BAS aMVECs. (**H**) Dose-response of PPARγ-UAS-bla HEK 293H cells exposed to ROSI and resolved with the same assay ($n = 4$). Bars represent mean ± SEM. Kruskal-Wallis test (**A**–**C** and **G**) and Wilcoxon's signed-rank test (**D** and **E**).

ine whether this effect was specific for ATGL, we silenced HSL. As shown in Supplemental Figure 3, suppression of HSL, in contrast with ATGL silencing, did not inhibit the positive effects of OA or GW9508. We conclude that ATGL, but not HSL, plays a critical role in aMVECs for FA-induced PPARγ and lipid transporter activation and, thus, for the induction of their endogenous and secreted PPARγ ligands.

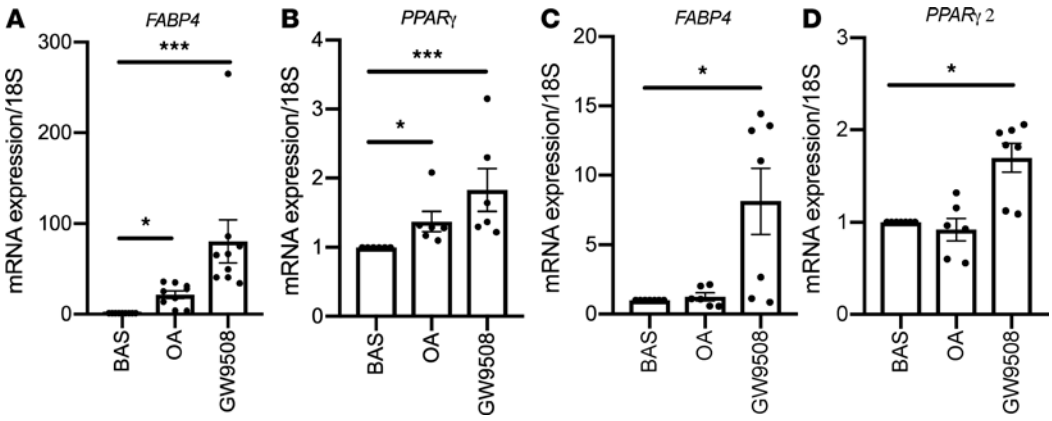

Figure 5. Effect of GRP40 ligand and OA in aMVECs and PAs. Cells were incubated for 24 hours without (BAS) or with 300 μM OA or 100 μM GW9508. qRT-PCR of FABP4 and PPARγ in aMVECs (**A** and **B**) or PAs (**C** and **D**). Data are from at least 6 experiments. *$P < 0.05$; ***$P < 0.001$ compared with BAS. Bars represent mean ± SEM. Kruskal-Wallis test.

aMVECs are unable to store large triglyceride droplets, indicating that lipids taken up by the cells need to be released continuously. As shown in Figure 7F, aMVECs cultured with OA for 24 hours accumulated many lipid droplets, and silencing ATGL further increased the number and size of the lipid droplets around 4-fold, supporting ATGL as an important regulator of continuous lipid degradation and activator of PPARγ in aMVECs and, subsequently, in adipocytes.

To further validate this, we performed coculture experiments with human PAs and aMVECs with or without prior silencing of ATGL in the aMVECs. As shown previously in Figure 4, D and E, aMVECs enhanced activation of PPARγ and FABP4 in PAs. Analogously, silencing ATGL in aMVECs markedly reduced transcriptional activation of *PPARγ*, *CD36*, and *FABP4* in PAs in the coculture experiments (Supplemental Figure 4). These findings corroborate the importance of the cross-talk between aMVECs and PAs in promoting PPARγ activation and the associated differentiation of the adipocytes and its regulation by ATGL in aMVECs.

Discussion

The adipose tissue is the main storage site for excess lipids and release of FAs as needed for energy homeostasis. PPARγ activation is essential for adipose precursor cells to undergo adipogenic differentiation (15) and to maintain their white phenotype through the cross-talk between zinc finger protein 423 and PPARγ (29–31). Murine cell lines, like 3T3-L1 cells, secrete their own ligands for PPARγ (15, 16). However, human adipose cells in vitro require external ligands for differentiation, and they undergo dedifferentiation if removed (17). This obviously cannot be the case in vivo, but how this is regulated is unknown. Several modified lipid species have been shown to activate PPARγ (32–34), but their physiological relevance is unclear.

The adipose tissue contains several different cells, and integrated communication between the cells is not unexpected. Recent studies showed that the adipose tissue is a major source of circulating exosomal miRNA targeting other tissues (10). Similarly, it was recently shown that murine endothelial cells release extracellular vesicles targeting the adipose cells in a glucagon- and sphingomyelinase-dependent system (9). We here show another distinct and important cross-talk, such that the adipose tissue endothelial cells regulate adipose cell lipid uptake and function through FA-dependent activation of PPARγ in the aMVECs and associated secretion of PPARγ ligand(s).

Human adipose tissue–derived endothelial cells have not been studied much previously, but a recent study showed that these cells are responsive to exogenous PPARγ ligands, leading to an increase in FA transporters, as we show here with FAs directly (20). It was also shown that senescence in these cells reduced their responsiveness to PPARγ ligands. We have also found that aMVECs can become senescent and are currently examining mechanisms and consequences for the adipose cells.

Using our previously described method to obtain purified aMVECs (26), we showed that they have an active transport of FA and that prolonged elevation of FA levels, as seen in obesity and T2D, induce a marked enhancement of their FA transport capacity and increase key FA-transporting proteins. This would obviously not only be related to external serum levels but also be following increased adipose cell lipolysis.

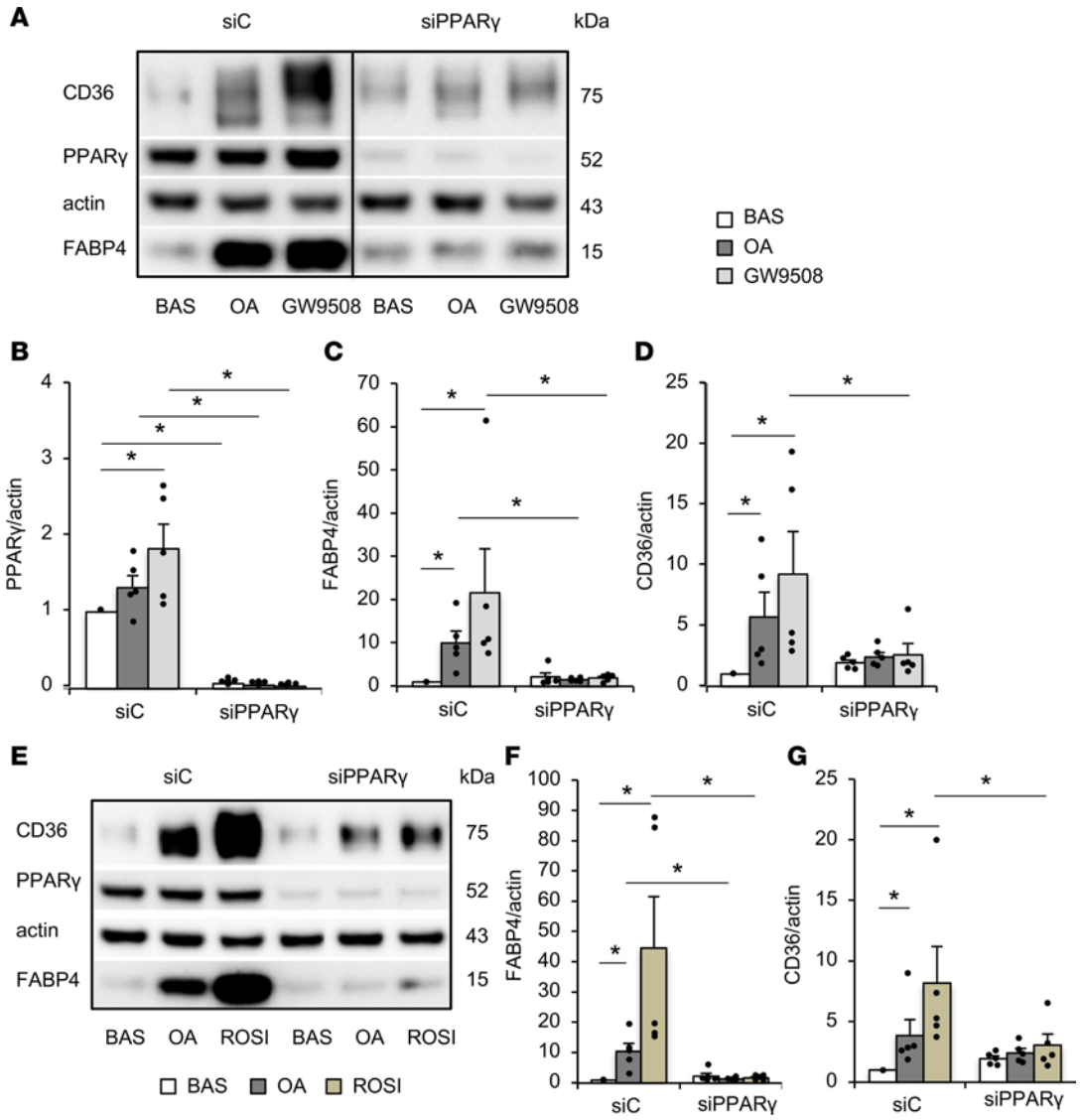

Figure 6. Suppressive effect of PPARγ siRNA. aMVECs were transfected with small interfering control (siC) or small interfering PPARγ (siPPARγ). Twenty-four hours after transfection, medium was changed to stimulation medium without (BAS) or with 300 μM OA or 100 μM GW9508 and incubated for an additional 24 hours. (**A**–**D**) Western blot analyses were performed using antibodies specific for CD36, PPARγ, FABP4, and actin, used as loading controls. (**A**) Western blots from 1 representative individual, and vertical lines represent removed and rejoined data from the same Western blot membrane. (**B**–**D**) Protein levels were analyzed by densitometry, and the bar histograms show protein levels of respective protein normalized to actin from 5 experiments. (**E**) Western blot membranes from 1 representative individual with the same conditions as above except that aMVECs were incubated with 5 μM ROSI. (**F** and **G**) Protein levels were analyzed by densitometry, and the bar histograms show protein levels of respective protein normalized to actin from 5 experiments. Bars represent mean ± SEM. Wilcoxon's signed-rank test, $^*P < 0.05$.

The effect of FAs was concentration and time dependent, required endogenous PPARγ activation, and was inhibited by different selective PPARγ antagonists and by genetic silencing of PPARγ. Consistent with this concept, mouse models with ubiquitous endothelial cell PPARγ deletion developed elevated lipid levels in the blood and had impaired uptake in peripheral tissues (18, 19). Thus, endothelial cell PPARγ is important for lipid transport and elimination to and from the blood in both human and murine cells. It has also been shown that endothelial cell CD36 acts as a gatekeeper for parenchymal FA uptake in the heart and skeletal muscle and that increased FA uptake in these tissues, not unexpectedly, reduces whole-body insulin sensitivity (35). In contrast, increased uptake and storage of FAs in the white adipose tissue should be protective for whole-body insulin sensitivity (36).

In contrast with aMVECs, human adipose precursor cells from the same donors did not respond to exogenous FAs with either PPARγ or FABP4 induction, consistent with the findings that these cells are dependent

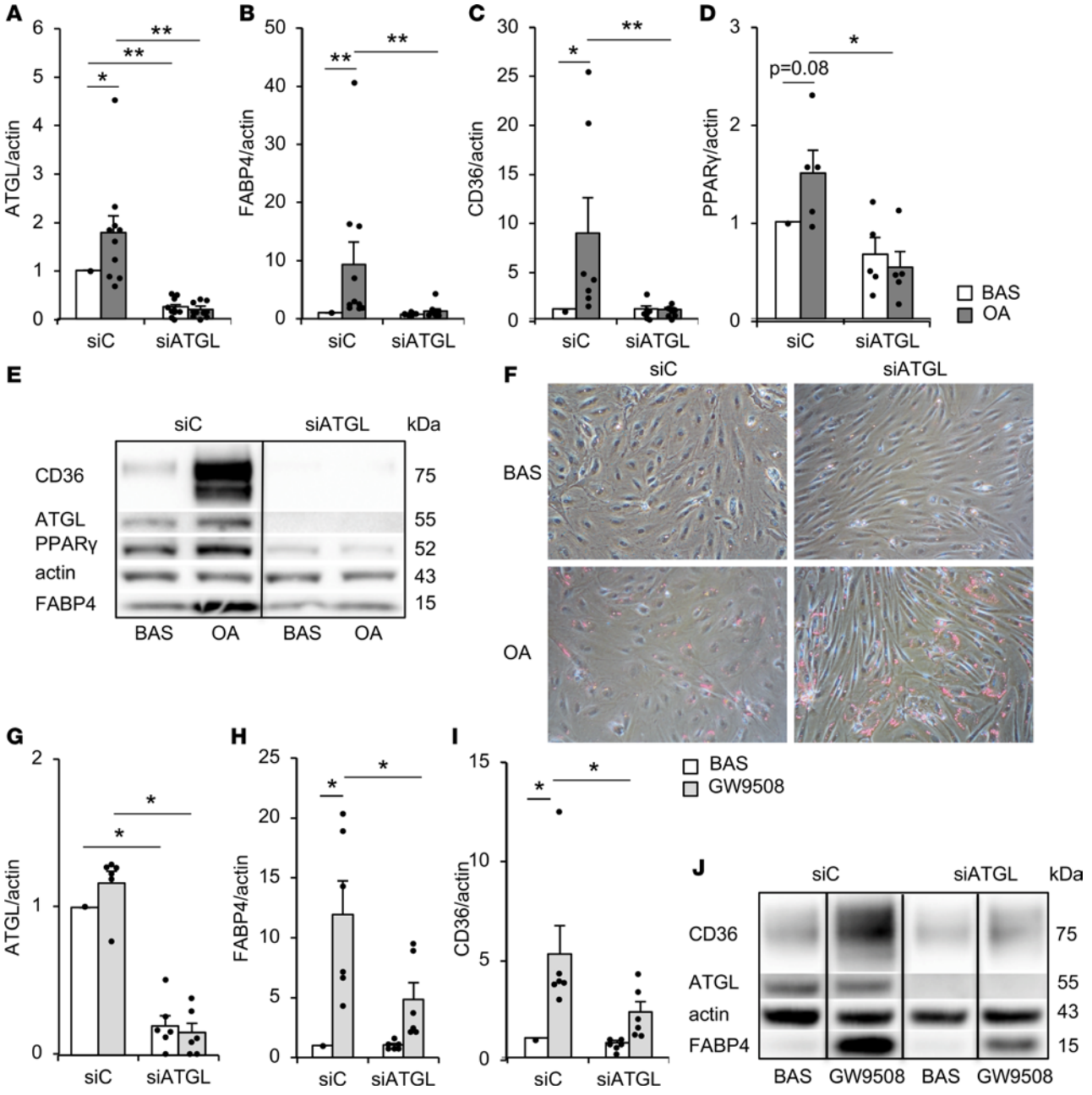

Figure 7. Suppressive effect of ATGL siRNA. aMVECs were transfected with siC or small interfering ATGL (siATGL). Twenty-four hours after transfection, medium was changed to stimulation medium without (BAS) or with 300 μM OA or 100 μM GW9508 and incubated for an additional 24 hours. (**A**–**D**) Western blots were performed using antibodies specific for ATGL, FABP4, CD36, PPARγ, and actin was used as a loading control. Protein levels were analyzed by densitometry, and the bar histograms show protein levels of respective proteins normalized to actin from at least 5 experiments. (**E**) The figure shows representative Western blots of CD36, ATGL, PPARγ, actin, and FABP4 in cells transfected with siC (left) or with siATGL (right). (**F**) Microphotographs of aMVECs transfected with RNA interference as described. Cells were treated without (BAS) or with 200 μM OA. The presence of lipids was revealed by Oil Red O staining (original magnification, ×100). (**G**–**I**) Western blots were performed as above, and data were obtained from at least 6 experiments. (**J**) Representative Western blots from the same membrane of CD36, ATGL, actin, and FABP4 for cells transfected with siC (left) or with siATGL (right). Vertical lines represent removed and rejoined data from the same Western blot membranes. Bars represent mean ± SEM. Wilcoxon's signed-rank test; $^{*}P < 0.05$; $^{**}P < 0.01$.

on exogenous PPARγ ligands (17). However, modified FAs developed as specific ligands for the FA receptor GPR40 (GW9508) exerted positive effects in both human adipose cells and aMVECs. Thus, both cell types respond to modified FAs whereas only aMVECs respond to nonmodified FAs as present in the bloodstream.

Long-term incubation of aMVECs with FAs enhanced lipid accumulation in the cells, but they never differentiated to adipose cells. Adipose precursor cells have been shown to reside in proximity to the vessel

cells, and endothelial cells have been postulated as adipose precursor cells (28). However, our data clearly show that mature aMVECs are not adipose precursor cells and cannot undergo adipogenic differentiation when exposed to a full differentiation cocktail. They do, however, accumulate lipid droplets when exposed to FAs and also respond to cAMP elevation by reducing their lipid content as a direct consequence of activating ATGL. Silencing ATGL for up to 72 hours increased their lipid accumulation, but the aMVECs cannot store large lipid droplets and, thus, can be susceptible to undergo lipid toxicity. These findings support the concept that ATGL plays an essential role in aMVECs by regulating their lipid accumulation and cell health.

An additional important finding was that ATGL-induced lipolysis, but not by HSL, is essential for the formation of endogenous and secreted lipids that activate PPARγ and the downstream PPAR-responsive FA transporter proteins in aMVECs. Furthermore, the adipose precursor cells responded to these secreted lipid(s) with increased PPARγ and FABP4 activation, showing the intimate cross-talk and dependence on aMVECs. Cocultures with aMVECs and PAs further documented the importance of functional ATGL in aMVECs in maintaining PPARγ activation and adipogenic differentiation, indicating that dysfunctional aMVECs in the adipose tissue may directly also lead to dysfunctional adipose cells.

We did not examine whether aMVECs also secreted ligands for PPARα following increased FA exposure. However, recent studies have shown that ATGL is important for the generation of ligands for PPARα in both the heart and liver (23–25). Thus, ATGL appears to have a particular role in the formation of modified lipids targeting the PPAR family in several tissues, and this effect is independent of any exogenous adrenergic stimulation or of HSL.

Even if aMVECs cannot become differentiated adipose cells, it is clear that they are highly specialized and resemble the adipose cells in several pathways related to lipid transport and accumulation. We also showed that aMVECs are different from both macrovascular HUVECs and microvascular cells derived from the heart in their gene regulation and ability to respond to FAs. This difference between endothelial cells is consistent with our previous findings that aMVECs do not respond to the amino acid metabolite 3-HIB, promoting FA uptake in skeletal muscle cells as well as in HUVECs and cMVECs (37). Thus, aMVECs have adopted a phenotype with specific advantages for their location as a barrier between blood and the adipose cells and with the ability to enhance lipid uptake, release, and storage/function in the adipose cells.

Finally, we showed here as well that the downstream effect of GPR40 ligands on FA transporters in aMVECs is dependent on ATGL. GPR40 has been shown to be an important downstream mediator of the effect of pioglitazone and other PPARγ ligands in human pulmonary endothelial cells (38). However, our data showed that this downstream effect in aMVECs is also dependent on ATGL and, thus, the formation of lipolytic products that enhance PPARγ activation (39).

Taken together, we showed here for the first time to our knowledge that human adipose tissue–derived endothelial cells are highly specialized and important regulators of adipose tissue lipid uptake and release and that they also cross-talk with the adipose cells to regulate PPARγ and ability to take up and store lipids. A priority is to identify the lipids aMVECs secrete and the mechanisms for the formation of PPAR ligands by ATGL. In this context, it should be added that several covalent modifications of FAs, including their nitration, have been shown to enhance the ability to activate PPARγ (38), but aMVECs essentially lack nitric oxide synthase 3 (26), making this an unlikely modification.

Methods

Source of adipose tissue. Human needle biopsies of the SAT were obtained from the abdominal region from 43 healthy donors and used to isolate aMVECs and the stromal vascular fraction containing PAs. The donors were 21 women and 22 men; had an average BMI (±SEM) of 27 (±0.9) and 27.4 (±0.8) kg/m^2, respectively; and were 50.6 (±2.4) and 43.8 (±2.7) years old, respectively.

aMVEC and PA isolation and culture. About 3 g adipose tissue was incubated in Medium199, Hanks' solution (Thermo Fisher Scientific), containing 4% BSA (Sigma-Aldrich) and 0.8 mg/ml collagenase (Sigma-Aldrich), at 37°C. The digest was filtered and washed with fresh medium as described previously (26). The fraction containing the stromal vascular cells was collected and cultured in an endothelial cell (EC) growth medium, EGM-2MV BulletKit (Lonza), consisting of EC basal medium-2 supplemented with EGM-2MV SingleQuot Kit (Lonza). The extraction of human aMVECs was performed with the Dynabeads magnetic CD31 MicroBeads cell sorting system (Thermo Fisher Scientific) as described previously (26). The positive selected ECs were resuspended in EC growth medium and cultured. The cells obtained with this procedure were 99% ECs with typical cobblestone morphology. Passages no higher than 8 were used for the experi-

ments. The $CD31^-$ cells with no beads attached included PAs and other stromal vascular cells, were removed during successive washings, and were collected and grown in DMEM:F12 (Lonza) supplemented with 10% FBS (Thermo Fisher Scientific) and penicillin/streptomycin (Thermo Fisher Scientific).

Cell culture conditions and collection of conditioned media. aMVECs, cMVECs (HMVEC-C, Lonza), and HUVECs (ATCC-CRL-1730, LGC Standards) were grown in EC growth medium or, for PAs, in DMEM:F12 supplemented as described. aMVECs, HUVECs, cMVECs or PAs were serum starved and incubated in their respective medium containing FA-free BSA (1 mg/ml) (Sigma-Aldrich) without (BAS) or with 300 μM OA (Sigma-Aldrich) or 5 μM ROSI (Sigma-Aldrich). For the conditioned media collection, the cells were grown as described above but in phenol red–free media. Aliquots of the collected media were used in the PPARγ reporter assay analysis. Other conditions are specified in figure legends. All the cells were free from mycoplasma contamination as assessed with MycoAlert Mycoplasma Detection Kit (Lonza).

PPARγ reporter assay. GeneBLAzer PPARγ-UAS-bla HEK 293H cells (Thermo Fisher Scientific) were plated in a 384-well black plate following the protocol provided by the supplier. aMVEC-conditioned media, obtained as described above, or naive media (control), were added to the cells and incubated for 20 hours. ROSI was used as a positive control. To determine the β-lactamase activity, CCF4-AM substrate–loading buffer (Thermo Fisher Scientific) was added to the cells and incubated in the dark. The plate was read in a fluorescence plate reader (Infinite F200 Tecan) using 409-nm excitation and 460-nm (blue) and 530-nm (green) emissions through the clear bottom of the plate. The data were plotted as a blue/green ratio (460 nm/530 nm) after background subtraction (medium only, without cells).

Adipogenic differentiation of adipose stromal cells. The human PAs were induced to differentiate, after 3 days of confluence, in DMEM:F12 supplemented with 3% FBS (Thermo Fisher Scientific), 850 nM insulin (Novo Nordisk), 10 μM dexamethasone (Sigma-Aldrich), 0.5 mM isobutylmethylxanthine (Sigma-Aldrich), and 10 μM pioglitazone (Sigma-Aldrich). After 3 days, the medium was changed to DMEM:F12 containing 10% FBS, 850 nM insulin, 1 μM dexamethasone, and 1 μM pioglitazone. The same differentiation cocktail but with EC growth medium was used for aMVEC differentiation.

aMVEC and adipocyte coculture and labeling with fluorescent BODIPY-500/510 C1, C12. aMVECs and PAs were grown independently either in cell culture dishes or in cell culture inserts, Thincerts (Greiner bio-one, BioNordika). The coculture design is illustrated in Figure 3, A and B. PAs were first differentiated into adipocytes as described above. The cells were used at differentiation days 7–10, when the lipids were visible under contrast microscopy. aMVECs were seeded and cultured in EC growth medium, to promote lipid accumulation, and the cells were exposed to 300 μM OA for 48 hours in serum-free EC growth medium containing FA-free BSA (1 mg/ml). For fluorescent-labeled lipids, the differentiated adipocytes and the aMVECs filled with lipids were incubated with 3 μM fluorescent long-chain FA analog BODIPY-500/510 C1, C12 (Thermo Fisher Scientific) for 3 hours, followed by a thorough wash of the label with PBS and subsequent addition of fresh medium. A second set of cells, differentiated adipocytes and non–OA-stimulated aMVECs with no fluorescent label, was also included in the coculture experiments (nonlabeled cells). The BODIPY-labeled and nonlabeled cells were paired as shown in Figure 3, A and B. BODIPY-labeled adipocytes were cocultured with unlabeled aMVECs, and BODIPY-labeled aMVECs were cocultured with unlabeled adipocytes. The microphotographs were taken after 48 hours of incubation with a Leica TCS SP5 microscope (Leica Microsystems).

Coculture aMVECs and PAs. Human primary PAs and aMVECs were separately seeded in Thincerts inserts or plates and cultured for 24 hours. After this period, inserts with aMVECs were added on top of the PAs or partially differentiated PAs, for 48 hours, and RNA was collected. Using the same coculture technique, additional experiments were performed with and without prior silencing of ATGL in the aMVECs.

FA uptake assay Quencher-Based Technology. The FA uptake was measured using the Quencher-Based Technology (QBT) Fatty Acid Uptake Assay Kit (Molecular Devices) according to the manufacturer's instructions. aMVECs were plated into a 96-well black-wall/clear-bottom plate at 10,000 cells/well. After 20 hours, the cells were stimulated without (BAS) or with 300 μM OA for 24 hours. Cells were then serum deprived for 1 hour, followed by the addition of QBT FA-loading buffer to each well. Kinetic readings were started immediately with the Infinite M200 fluorescence plate reader (Tecan). Instrument settings were bottom read, excitation 488/emission 515, with a filter cutoff at 495 nm.

Oil Red O staining. Before staining, the cells were fixed for 10 minutes in 4% formaldehyde (Histolab) and washed with PBS. The cells were incubated with filtered Oil Red O (O-R-O) (Sigma-Aldrich) working solution for 20 minutes. The cells were counterstained with hematoxylin (Histolab).

Quantification of images in ImageJ. Lipid accumulation was quantified for the amount of O-R-O staining by the image-dedicated software ImageJ (NIH). The estimate of O-R-O was obtained by using pixel numbers as the quantitative measurement. The results expressed as RawIntDen represent the sum of all values of all pixels in the image.

RNA interference. aMVECs were transfected with siRNA directed against *ATGL* (Hs01 00225605 and Hs01 00225606; Sigma-Aldrich), PPARγ (Hs01 00218390 and Hs01 00218391), HSL (Hs01 00175631), or MISSION siRNA Universal Negative Control (SIC001; Sigma-Aldrich). Briefly, cells were transfected with 30 nmol/l siRNA by using Lipofectamine RNAiMAX (Thermo Fisher Scientific) according to the manufacturer's instructions using 12-well plates.

RNA extraction and qRT-PCR. RNA was isolated with the E.Z.N.A. Total RNA Kit (Omega Bio-tek), and cDNA synthesis was done using the High Capacity cDNA Reverse Transcription Kit (Thermo Fisher Scientific). qRT-PCR was performed using the ABI PRISM 7900HT Sequencing Detection System or the QuantStudio6 Flex System (Thermo Fisher Scientific). Relative quantities of target transcripts were calculated from duplicate samples after normalization of the data against the endogenous control, human 18S rRNA (Thermo Fisher Scientific). Primers and probes were designed using the Primer Express software (Supplemental Table 1) or purchased as Assay-on-Demand for PPARg (Hs00234592_m1), CD36 (Hs00169627_m1) or FABP4 (Hs01086177_m1) (Thermo Fisher Scientific).

Whole-cell extracts and Western blot analyses. Whole-cell protein lysates were prepared and Western blot analyses were performed as previously described (40). Briefly, protein concentration was determined using the Pierce BCA Protein Assay Kit (Thermo Fisher Scientific), and 5–15 μg whole-cell extracts were loaded on NuPAGE Novex 4%–12% Bis-Tris protein gels (Thermo Fisher Scientific). The Trans-Blot Turbo Transfer System (Bio-Rad) was used for protein transfer, and to ensure that the procedure had been fully completed, the membranes were colored using 0.5% Ponceau S (Merck Chemicals). The quantification of protein expression was based on a minimum of 4 replicates, and for the detection of specific proteins, the following primary antibodies were used: anti-FABP4 (AF1443 or MAB3150, R&D Systems), anti-PPARγ (2443, Cell Signaling Technology), anti-CD36 (14347, Cell Signaling Technology, or ab17044, Abcam), anti-ATGL (sc-67355, Santa Cruz Biotechnology), anti-HSL (4107, Cell Signaling Technology), anti-actin (sc-8432, Santa Cruz Biotechnology), and HRP-conjugated secondary antibodies anti–rabbit IgG (catalog 7074), anti–mouse IgG (catalog 7076), and anti–rat IgG (catalog 7077) from Cell Signaling Technology and anti–goat IgG (sc-2020) from Santa Cruz Biotechnology.

Statistics. The statistical analyses were performed using GraphPad Prism 8 or SPSS Statistics software. Normal data distribution was determined using Shapiro-Wilk test. Student's two-tailed *t* test or Wilcoxon's signed-rank test was performed for paired comparisons and 1-way ANOVA or Kruskal-Wallis test for multiple value comparisons. Data analyses are presented as mean ±SEM. The different tests were used as specified in the figure legends. *P* value less than 0.05 was considered significant.

Study approval. All participants were informed and provided written consent before taking part in the study, which was approved (dnr. 151-14) by the Ethics Committee of the University of Gothenburg, Gothenburg, Sweden.

Author contributions

SG, AN, and US designed the studies. SG and AN performed experiments and analyzed data. Results were interpreted by SG, AN, and US. The manuscript was written by US, SG, and AN with input from JB. All authors reviewed the results and approved the final version of the manuscript.

Acknowledgments

These studies were supported by grants from the Swedish Research Council, Torsten Söderberg Foundation (M58/16), Swedish Diabetes Foundation (DIA2017-206), and Novo Nordisk Foundation (NNF17OC0026712). The funders had no influence on the work performed.

Address correspondence to: Ulf Smith, Lundberg Laboratory for Diabetes Research, Department of Molecular and Clinical Medicine, Sahlgrenska Academy at the University of Gothenburg, Blå Stråket 5, 41345 Gothenburg, Sweden. Phone: 46313421104; Email: ulf.smith@medic.gu.se.

1. Gustafson B, Hedjazifar S, Gogg S, Hammarstedt A, Smith U. Insulin resistance and impaired adipogenesis. *Trends Endocrinol Metab*. 2015;26(4):193–200.

2. Rosen ED, Spiegelman BM. What we talk about when we talk about fat. *Cell*. 2014;156(1–2):20–44.
3. Smith U, Kahn BB. Adipose tissue regulates insulin sensitivity: role of adipogenesis, de novo lipogenesis and novel lipids. *J Intern Med*. 2016;280(5):465–475.
4. Després JP, Lemieux I. Abdominal obesity and metabolic syndrome. *Nature*. 2006;444(7121):881–887.
5. Zamarron BF, et al. Macrophage proliferation sustains adipose tissue inflammation in formerly obese mice. *Diabetes*. 2017;66(2):392–406.
6. Nishimura S, et al. Adipogenesis in obesity requires close interplay between differentiating adipocytes, stromal cells, and blood vessels. *Diabetes*. 2007;56(6):1517–1526.
7. Cao Y. Angiogenesis modulates adipogenesis and obesity. *J Clin Invest*. 2007;117(9):2362–2368.
8. Barnhart KF, et al. A peptidomimetic targeting white fat causes weight loss and improved insulin resistance in obese monkeys. *Sci Transl Med*. 2011;3(108):108ra112.
9. Crewe C, et al. An endothelial-to-adipocyte extracellular vesicle axis governed by metabolic state. *Cell*. 2018;175(3):695–708.e13.
10. Thomou T, et al. Adipose-derived circulating miRNAs regulate gene expression in other tissues. *Nature*. 2017;542(7642):450–455.
11. Hamilton JA. New insights into the roles of proteins and lipids in membrane transport of fatty acids. *Prostaglandins Leukot Essent Fatty Acids*. 2007;77(5-6):355–361.
12. Jay AG, Hamilton JA. The enigmatic membrane fatty acid transporter CD36: New insights into fatty acid binding and their effects on uptake of oxidized LDL. *Prostaglandins Leukot Essent Fatty Acids*. 2018;138:64–70.
13. Hagberg CE, et al. Vascular endothelial growth factor B controls endothelial fatty acid uptake. *Nature*. 2010;464(7290):917–921.
14. Van der Vusse GJ, Glatz JF, Van Nieuwenhoven FA, Reneman RS, Bassingthwaighte JB. Transport of long-chain fatty acids across the muscular endothelium. *Adv Exp Med Biol*. 1998;441:181–191.
15. Tontonoz P, Spiegelman BM. Fat and beyond: the diverse biology of PPARγ. *Annu Rev Biochem*. 2008;77:289–312.
16. Tzameli I, et al. Regulated production of a peroxisome proliferator-activated receptor-γ ligand during an early phase of adipocyte differentiation in 3T3-L1 adipocytes. *J Biol Chem*. 2004;279(34):36093–36102.
17. Gustafson B, Smith U. The WNT inhibitor Dickkopf 1 and bone morphogenetic protein 4 rescue adipogenesis in hypertrophic obesity in humans. *Diabetes*. 2012;61(5):1217–1224.
18. Kanda T, et al. PPARγ in the endothelium regulates metabolic responses to high-fat diet in mice. *J Clin Invest*. 2009;119(1):110–124.
19. Goto K, et al. Peroxisome proliferator-activated receptor-γ in capillary endothelia promotes fatty acid uptake by heart during long-term fasting. *J Am Heart Assoc*. 2013;2(1):e004861.
20. Briot A, et al. Senescence alters PPARγ (Peroxisome Proliferator-Activated Receptor Gamma)-dependent fatty acid handling in human adipose tissue microvascular endothelial cells and favors inflammation. *Arterioscler Thromb Vasc Biol*. 2018;38(5):1134–1146.
21. Zimmermann R, et al. Fat mobilization in adipose tissue is promoted by adipose triglyceride lipase. *Science*. 2004;306(5700):1383–1386.
22. Young SG, Zechner R. Biochemistry and pathophysiology of intravascular and intracellular lipolysis. *Genes Dev*. 2013;27(5):459–484.
23. Haemmerle G, et al. ATGL-mediated fat catabolism regulates cardiac mitochondrial function via PPAR-γ and PGC-1. *Nat Med*. 2011;17(9):1076–1085.
24. Jha P, et al. Role of adipose triglyceride lipase (PNPLA2) in protection from hepatic inflammation in mouse models of steatohepatitis and endotoxemia. *Hepatology*. 2014;59(3):858–869.
25. Khan SA, Sathyanarayan A, Mashek MT, Ong KT, Wollaston-Hayden EE, Mashek DG. ATGL-catalyzed lipolysis regulates SIRT1 to control PGC-1α/PPAR-α signaling. *Diabetes*. 2015;64(2):418–426.
26. Gogg S, Smith U, Jansson PA. Increased MAPK activation and impaired insulin signaling in subcutaneous microvascular endothelial cells in type 2 diabetes: the role of endothelin-1. *Diabetes*. 2009;58(10):2238–2245.
27. Hagberg CE, et al. Targeting VEGF-B as a novel treatment for insulin resistance and type 2 diabetes. *Nature*. 2012;490(7420):426–430.
28. Gupta RK, et al. Zfp423 expression identifies committed preadipocytes and localizes to adipose endothelial and perivascular cells. *Cell Metab*. 2012;15(2):230–239.
29. Min SY, et al. Human 'brite/beige' adipocytes develop from capillary networks, and their implantation improves metabolic homeostasis in mice. *Nat Med*. 2016;22(3):312–318.
30. Longo M, et al. Epigenetic modifications of the Zfp/ZNF423 gene control murine adipogenic commitment and are dysregulated in human hypertrophic obesity. *Diabetologia*. 2018;61(2):369–380.
31. Shao M, et al. Zfp423 maintains white adipocyte identity through suppression of the beige cell thermogenic gene program. *Cell Metab*. 2016;23(6):1167–1184.
32. Ahmed W, et al. PPARs and their metabolic modulation: new mechanisms for transcriptional regulation? *J Intern Med*. 2007;262(2):184–198.
33. Hallenborg P, Petersen RK, Kouskoumvekaki I, Newman JW, Madsen L, Kristiansen K. The elusive endogenous adipogenic PPARγ agonists: Lining up the suspects. *Prog Lipid Res*. 2016;61:149–162.
34. Marion-Letellier R, Savoye G, Ghosh S. Fatty acids, eicosanoids and PPAR gamma. *Eur J Pharmacol*. 2016;785:44–49.
35. Son NH, et al. Endothelial cell CD36 optimizes tissue fatty acid uptake. *J Clin Invest*. 2018;128(10):4329–4342.
36. Hammarstedt A, Gogg S, Hedjazifar S, Nerstedt A, Smith U. Impaired adipogenesis and dysfunctional adipose tissue in human hypertrophic obesity. *Physiol Rev*. 2018;98(4):1911–1941.
37. Mardinoglu A, et al. Elevated plasma levels of 3-hydroxyisobutyric acid are associated with incident type 2 diabetes. *EBioMedicine*. 2018;27:151–155.
38. Wang S, et al. G protein-coupled receptor 40 (GPR40) and peroxisome proliferator-activated receptor γ (PPARγ): An integrated two-receptor signaling pathway. *J Biol Chem*. 2015;290(32):19544–19557.
39. Wang S, Dougherty EJ, Danner RL. PPARγ signaling and emerging opportunities for improved therapeutics. *Pharmacol Res*. 2016;111:76–85.
40. Gustafson B, Smith U. Cytokines promote Wnt signaling and inflammation and impair the normal differentiation and lipid accumulation in 3T3-L1 preadipocytes. *J Biol Chem*. 2006;281(14):9507–9516.